Journal of Power Sources 250 (2014) 286–295

Contents lists available at ScienceDirect

Journal of Power Sources

journal homepage: www.elsevier.com/locate/jpowsour

Development and realization of a hydrogen range extender hybrid city bus

F. Sergi*, L. Andaloro, G. Napoli, N. Randazzo, V. Antonucci

Institute of Advanced Energy Technologies "Nicola Giordano", National Research Council of Italy, Salita S. Lucia Sopra Contesse, 5, 98126 Messina, Italy

HIGHLIGHTS

- To increase the range of the vehicle a range extender powertrain configuration was chosen.
- The powertrain is composed by a FC system, Zebra batteries and an AC induction motor.
- The control strategy adopted allows to assure the functionality of the vehicle.

ARTICLE INFO

Article history:
Received 9 August 2013
Received in revised form
30 October 2013
Accepted 1 November 2013
Available online 20 November 2013

Keywords:
Fuel cell vehicles
Hybrid powertrain
Range extender
Urban mobility

ABSTRACT

Electric vehicles, equipped with electrochemical batteries, are expected to significantly penetrate the automotive market in the next few years. Though, the recharge time for battery pack and the autonomy range can constitute a limit. An appropriate use of fuel cell technology in electric vehicles can now represent an advantageous choice both from a technical and economic point of view.

This paper reports the results of the development of a hybrid electric city bus, performed by the synergy between fuel cell and batteries. A pure electric city bus, equipped with eight Zebra batteries, was acquired and modified in a fuel cell and batteries hybrid vehicle. In the final version the bus was equipped with six batteries and a hydrogen plant with a proton exchange membrane fuel cell system. In particular an innovative powertrain management, where even the time required for the terminal stops is used to charge the batteries by the fuel cell, is described. Set-up tests on the fuel cell system acquired are presented. Further, tests were conducted also on the battery pack working on board in a real route to demonstrate the capability of the reduced battery pack to drive the vehicle.

1. Introduction

The swift growth of the global population is concentrating in urban areas, determining an increasing consumption of energy due to cities. Given that, specific energy policies related to urban areas are already foreseen with the aim at reducing energy consumption, increasing energy efficiency and mitigating the CO_2 emissions. In this contest, mobility and transportation can be considered one of the key elements to achieve these targets. Furthermore, long term petrol price increases and climate changes have created in the automotive industry a new competitive market based on the spread of more sustainable technologies.

Several automotive manufacturers have promoted interest in full electric vehicles (EVs) and hybrid vehicles (HVs) because both types of means of transportation could be run comparable with traditional fuelled vehicles but are more cheaper to maintain and environmentally friendly [1–3]. Given that, the urban mobility is a key issue to improve the life quality of people, to increase market opportunities, and to achieve a more sustainable transportation of goods and people [4,5].

The actual early market is based on the commercialization of HVs provided with internal combustion engine (ICE) and electric motors supplied by batteries. Battery, depending on the rate of power of the electric motor with respect the ICE, is used for regenerative breaking and for the traction at low speed (urban centres). This approach allows reducing the fuel consumption and CO_2 emissions, but does not avoid the presence of hydrocarbons. The pure EVs, that do not present any ICE in the powertrain, due to their limited autonomy range, are expected to cover the market segment of city cars and city buses [6]. Nowadays, hydrogen technologies are considered too expensive both for the costs of fuel cell systems (FCS) and hydrogen. Further the life time (40,000 h) of the FCS has to be improved.

Within an Italian national project, CNR-ITAE is involved in the development of a hybrid electric city bus, composed by the hybridization between fuel cell and batteries able to overcome the

* Corresponding author. Tel.: +39 090 624241; fax: +39 090 624247.
E-mail address: francesco.sergi@itae.cnr.it (F. Sergi).

0378-7753/$ – see front matter © 2013 Elsevier B.V. All rights reserved.
http://dx.doi.org/10.1016/j.jpowsour.2013.11.006

limits of individual technologies through the synergy of the two systems [7]. The final prototype aims to demonstrate that an appropriate use of fuel cells in electric vehicles can perform, yet now, a real competitive product, above all if employed in vehicles fleets.

2. Background

A pure electric city bus was acquired and converted in a fuel cell hybrid city bus.

The project targets are reported below:

- increasing the overall autonomy (+30%) respect the electric version
- keeping low the cost of investment through the use of a reduced size of fuel cell system
- minimizing the time for the batteries recharge
- keeping the initial number of passengers and the same weight

To achieve these goals, a range extender powertrain configuration was chosen. The FCS through the DC/DC step up converter works in parallel with battery pack, and both supply energy to the DC side of the motor inverter [8]. The principal energy source is the battery pack. The FCS, working at constant power, pushes the State of Charge (SoC) of the batteries during the bus stops, but is used also during the traction.

The vehicle selected for the prototype realization is a city bus (Model Alè Elettrico, Rampini Carlo SPA) of 44 passengers capacity and a AC drive motor of 85 kW (rated power) with regenerative breaking system (Fig. 1).

A preliminary design and dimensioning were carried out on the basis of energy aspects using simulation models developed in Simulink environment and more details can be found in Ref. [9].

The optimal level of hybridization was evaluated as reported in Refs. [9], and consists of a low power fuel cell system and 6 Zebra batteries [10–14]. The PEM system, installed on the roof of the bus, is fed by hydrogen stored in 2 tanks (Dynetec, compressed at 200 bar) containing about 4.8 kg of hydrogen each [15]. With this configuration the project targets can be achieved. The comparison of the capital cost between the only-battery version and the hybrid one is 15% more, considering the reduced battery pack and the additional costs due to the whole hydrogen plant. So, the hybrid version cost is a little bit more than the only battery version.

Fuel cost prediction needs to take into account the targets for the next years of hydrogen prices and the way to produce (from natural gas or from renewables), to store and distribute it in the future. Cost analysis has to consider several aspects from now to the next 10–20 years: hydrogen infrastructures spread, large scale use, improvement and cost reduction of hydrogen technologies [16]. Considering the target of 3,5 $ kg^{-1} [17], the cost prediction for this vehicle, due to hydrogen, should be about 33 $ per day.

This range-extender configuration proposed can now:

- reduce the number of vehicles needed in an electric buses fleet management, thanks to the fast refueling due to the hydrogen and to the extended autonomy
- facilitate the creation of a hydrogen vehicles early market thanks to the lower investment cost, compared with the full power one (total fuel cell vehicle)

Taking in to account that the hydrogen pressure in this bus was set at 200 bar (the available hydrogen refueling is @ max 250 bar), other additional advantages (more autonomy) due to an enhanced fuel compression (350 bar), could be obtained by the same powertrain, without a vehicle weight growth.

Fig. 1. Hybrid city bus developed.

3. Powertrain management

3.1. Electrical architecture

The powertrain (Fig. 2) is composed by:

- Six ZEBRA batteries (Model Z5-557-ML3X-38 – FZSonick, Rated Energy: 21.1 kWh, OCV: 557 V, Efficiency: 90%), divided in two sub battery packs of three batteries each one. The first was installed inside the city bus, the second in the rear.
- A fuel cell system (Model PFV005 Nuvera Fuel Cells, Nominal Power: 5 kW, 40 cells in series, Efficiency: 55%) positioned on the roof of the bus jointly the hydrogen storage systems (design developed by SOL).
- A DC/DC step-up converter developed during the project by STMicroelectronics (Nominal Power: 6 kW, Efficiency: 89%).
- The previous traction section, represented in Fig. 2 by the AC induction motor (Model 1PV5138-4WS24, Siemens) and the 3 phases inverter (Model DC-DC/IGBT MONO Inverter, Siemens).

In Fig. 2 the scheme reports also the connections with the auxiliary services section, where a DC/DC Step-down converter allows recharging the 24 V aux battery and supplying the services during the traction. When the ZEBRA traction batteries are not already activated, the 24 V aux battery performs the switching-on

Table 1
City bus configuration.

Parameter	Unit	Value
Bus weight	kg	10904
Bus dimensions	mm	7570 × 2200 × 3120
Bus n_{seats}	–	44
Bus electrical engine	kW	85
Bus Vnom, DC	V	650
Bus Vop, DC	V	300–750
Fuel cell system power	kW	5.6
Fuel cell system output voltage	V	27–40
Fuel cell DC–DC converter voltage (nominal)	V	36_{down} – 600_{up}
Fuel cell DC–DC converter power (nominal)	kW	6
Cylinder volume	l	150
Number of cylinders	–	2
Cylinders pressure	bar	200
Hydrogen mass	kg	4.89
Single battery energy	kWh	21,2
Single battery power	kW	30
Number of batteries	–	6

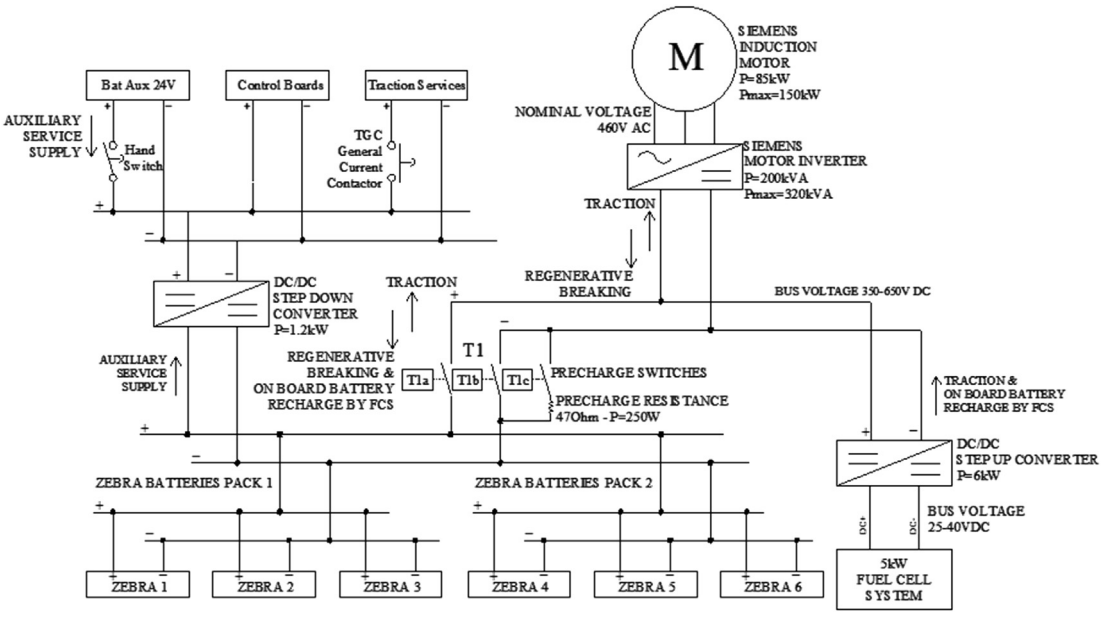

Fig. 2. Electrical architecture of the powertrain.

of the city bus. The TGC (General Current Contactor) and the Hand Switch can be considered the main switches of the bus. The city bus configuration is reported in Table 1.

A pre-charge resistance was foreseen to prevent excessive inrush current during the powering of the DC-Link. As a matter of fact big capacitances are present in the DC input side of inverter and in the output side of the DC/DC Step-up Converter. The charge and discharge of these capacitances has to be managed in order to limit the current for safeguarding T1 switch. The switching sequence of $T1_a$. $T1_b$ and $T1_c$ starts when the DC link of battery pack is already activated. When $T1_c$ is switched, the current flows from batteries to the traction section, through the 47 Ohm resistance.

During the traction, the DC-Link among FCS, Battery, and traction section is managed by the battery output voltage (350–557 V – Discharge). During regenerative breaking, the DC side of the Siemens inverter imposes a regenerative voltage to the battery DC link; the voltage rises assuring the charge of the battery. The voltage limitation is send by battery on Vehicle CAN.

3.2. DC/DC step-up converter development

The DC–DC step-up converter is actually under development. It works pushing the output voltage of fuel cell system from 27 to 40 V up to the DC link Voltage (550 nominal voltage) and regulating the output power of FCS at constant value (5.6 kW). In these conditions the Proton Exchange Membrane fuel cell system operates at constant power every time the power required by the motor and auxiliary systems is greater than 5.6 kW, preserving it from continuous changes in the operating point. The working point is positioned in the ohmic region @ 0.6 V/cell (polarization curve). It is

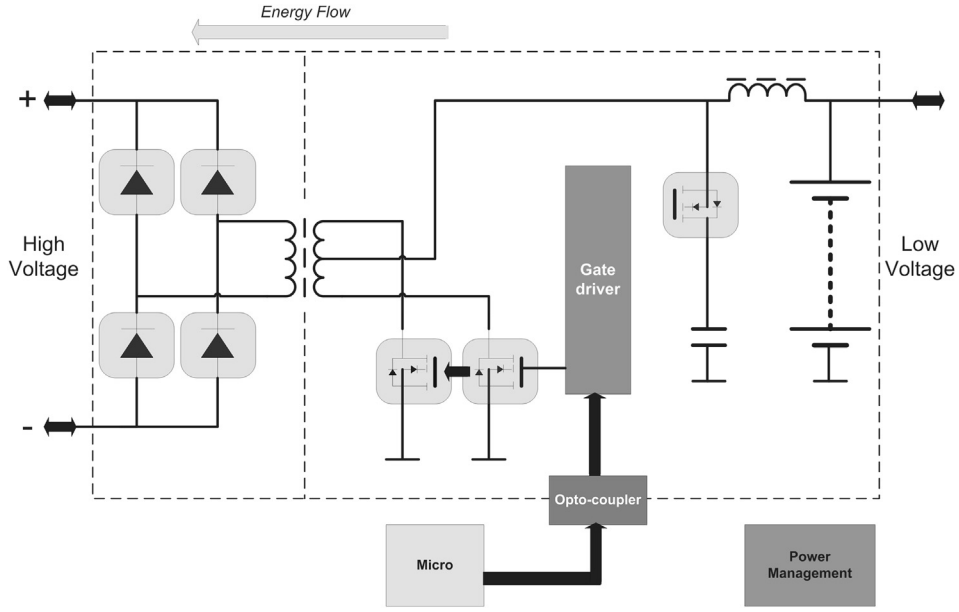

Fig. 3. DC/DC converter topology.

well known that potential values play an important role during the P_t degradation process. Higher potentials can accelerate P_t dissolvability [18]. The concentration of dissolved P_t increases monotonically from 0.65 to 1.1 V/cell [19], so the chosen working point mitigates P_t degradation processes. Moreover, carbon corrosion can also arise from a non-uniform distribution of fuel on the anode side (partial hydrogen coverage) and from crossover of reactant gas through the membrane. Both start-up and shutdown can cause this type of carbon corrosion [20]. Only one FCS start-up and shutdown per day were foreseen, because the cell works ever @ 5.6 kW both during the urban route and during the terminal stops (on board battery recharge).

The galvanic insulated DC/DC converter was designed in order to control voltage and current output. It is divided in two modules (low voltage and high voltage) performed with a *push–pull* topology [21], each of them foresees a couple of transistors in the input, a transformer and a diode bridge to rectify the output voltage (Fig. 3).

The micro controller generates 8 PWM (Pulse with Modulation) signals for each module, four are used for piloting the Power MOSFET, and four for the active clamps to protect the devices from voltage spikes. Starting from the BUS voltage acquisition, it is calculated the current reference that each module musts follow (Fig. 4). The control strategy is based on the implementation of two PI (Proportional Integrative) regulators (provided with an independent dynamic) that adjust the duty cycle of the own PWM, depending on the difference between the measured current and the reference current (error). The reference current, obtained by the output voltage and reference power (send by CAN), cannot exceed the 5 A limit for each module. This avoids excessive currents in the case of low output voltage.

The power set points of the DC–DC Converter (P_{DC-DC}), and consequently of the fuel cell system, are decided by Master controller (message send by CAN to the DC–DC Converter), depending on three different conditions:

- $P_{DC-DC} = 1.5$ kW only in the case of overcharge of the battery pack (SoC>100%). It was calculated that 1.5 kW can be absorbed by the vehicle subsystems.
- $P_{DC-DC} = 2.5$ kW only during the warm-up of fuel cell system. As long as the cathode water temperature doesn't reach 38 °C, the polymeric membrane is not considered well humidified by the control unit. So the FCS output power is limited @ 2.5 kW to prevent excessive initial currents during warm-up.
- $P_{DC-DC} = 5$ kW ever, in all other cases.

Several error types were defined to safeguard the device (Table 2).

When these errors (Boolean) are active, the generation of PWM signals is stopped.

Table 2
DC/DC error list.

ERR_OVER_VOLTAGE_OUT	DC/DC voltage output above *Sys_voltageMaxGenerator* or *Sys_voltageMaxCharge*
ERR_OVER_LOAD	Output current above 5 A for each module
ERR_OVER_TEMP	Temperature above 80 °C
ERR_OVER_VOLTAGE_IN	DC/DC voltage input above 40 V
ERR_UNDER_VOLTAGE_IN	DC/DC voltage input below 25 V

The operation range of the errors is parameterized, except for ERR_OVER_VOLTAGE_OUT.

The voltage limit is managed by the battery pack. As a matter of fact, concerning this issue, MBS sends on vehicle CAN two CAN messages: *sys_voltageMaxGenerator* and *sys_voltageMaxCharge*, that constitute the voltage targets for the converter:

- *Sys_voltageMaxGenerator* during the traction (traction is the normal operation of the vehicle)
- *Sys_voltageMaxCharge* during regenerative breaking (this state is achieved when the *Drive_Motor_Torque*, coming from the SIEMENS engine, changes its status). The Boolean *sys_regenBrakingEnable*, coming from MBS has to be 1.
- *Sys_voltageMaxCharge* during the terminal stops (this state is achieved when MC sends *LINE_CHARGE* on *MC_STATES_Actual* variable).

The value of *sys_voltageMaxGenerator* depends on the state of charge of the battery pack (Fig. 5).

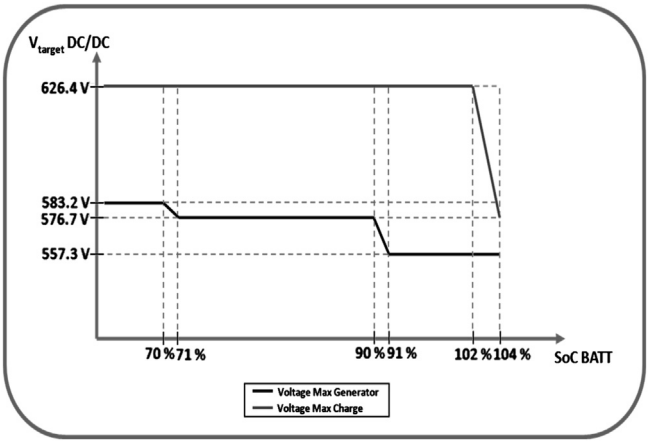

Fig. 5. Battery voltage limitation.

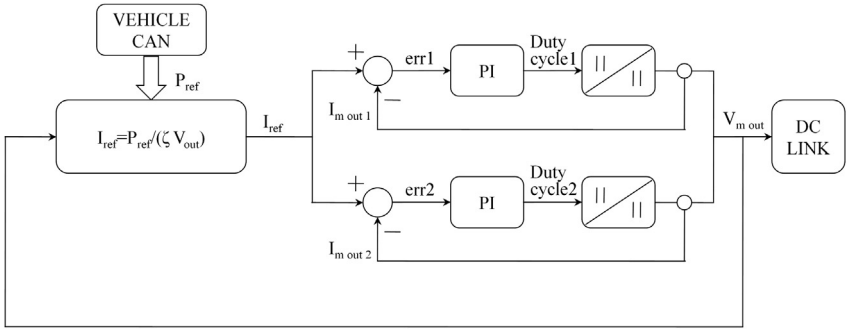

Fig. 4. DC/DC control scheme.

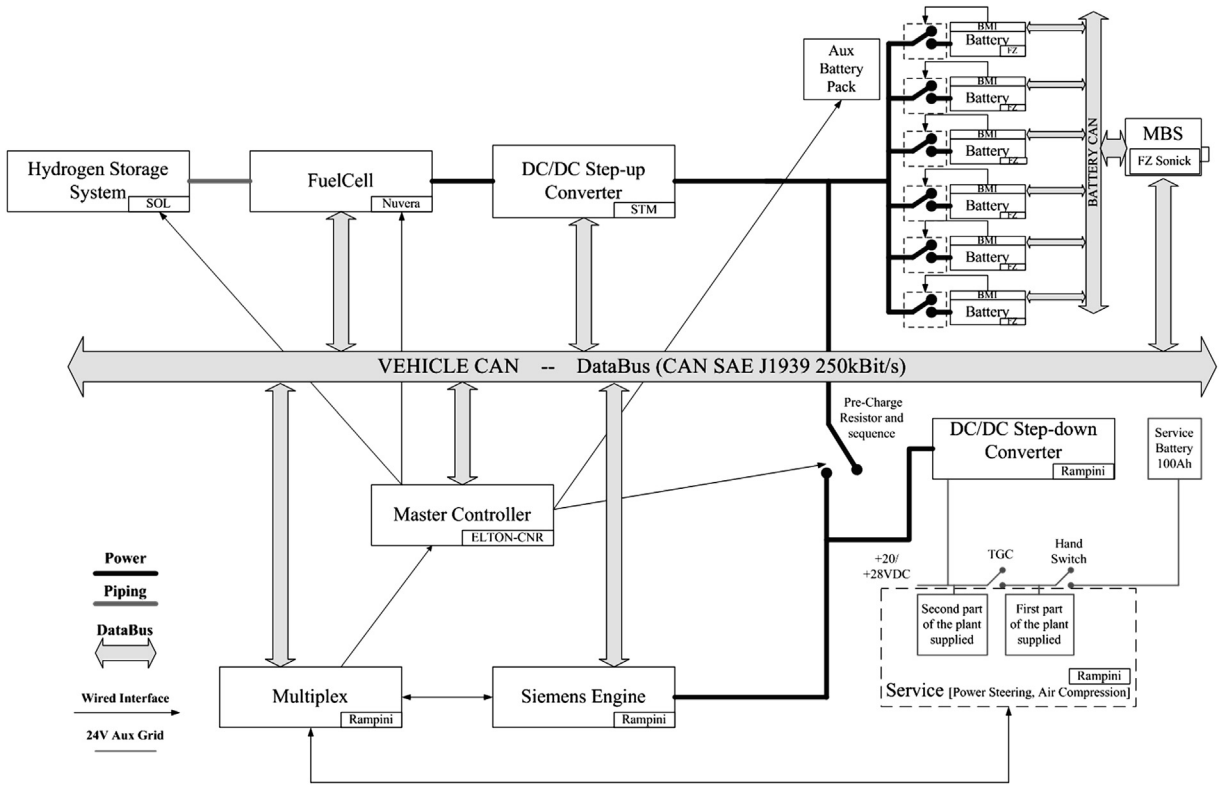

Fig. 6. City bus control architecture.

Regenerative braking is possible during battery discharge. The threshold value *sys_voltageMaxGenerator* is calculated as a function of SOC. All values of battery voltage above *sys_voltageMaxGenerator* are considered as regenerative braking.

Regenerative braking has to be reduced if $\Delta SOC_{regen} > 2\%$ and will be reset after a depolarisation discharge.

$$U_{bat} > Sys\_voltageMaxGenerator(\text{regenerative braking})$$

is calculated as following:

$$0 \leq \Delta SOC_{regen} \leq 4\%$$

SOC_{regen} is computed in charge if $U_{bat} >$ V max generator.

If the battery is charged by ΔSOC

$$(I_{bat} < 0,\ \text{charging}) \text{and} (U_{bat} > sys\_VoltageMaxGenerator)$$

$$\Delta SOC_{regen} = \Delta SOC_{regen} + \Delta SOC$$

If the battery is discharged by ΔSOC

$$(I_{bat} > 0,\ \text{discharging},\ \text{minimum discharge 10 A})$$

$$\Delta SOC_{regen} = \Delta SOC_{regen} - \Delta SOC{*}60$$

If $\Delta SOC_{regen} > 2\%$ a limitation applies, maximum limitation is set with $\Delta SOC_{regen} = 4\%$.

Limitations depend on both battery SOC and ΔSOC_{regen}, a limitation applies if $\Delta SOC_{regen} > 2\%$.

Maximum limitation (regenerative braking is disabled) is set with $\Delta SOC_{regen} = 4\%$.

A limitation applies if SOC > 102%. Maximum limitation (regenerative braking is disabled) is set with SOC = 104%.

Therefore, different values of voltage limit for the DC/DC step-up converter are defined. The difference between the actual voltage and the "charge voltage", depending on the internal resistance of the battery (it is a function of the SoC) determines the "charge current" by the DC/DC Converter. The current limit is also defined by another CAN message by the MBS: *sys_currentMaxCharge*.

3.3. Master controller

A dedicated supervisor, Master controller (MC), was developed to control the integration and functionality of the new devices installed in the bus. The MC works at a superior level compared to the previous control system (called Multiplex) whose functions are concerning the control of the service equipment, Siemens engine and previous logic implemented.

MC, equipped with several digital and analogue I/O and with 3 CAN BUS gateways (SAE J1939 250 kbit/sec), through a dedicated software, manages the operation of the bus, and in particular the Start-up, the Shut-down, and all the procedures coming from warnings and faults. Digital I/O are used especially for the contactors management; analogue I/O for the control of the hydrogen storage system (acquisition of temperatures, pressures, flows, etc.) and for the wired controls.

The scheme in Fig. 6 reports the connections among the main equipment of the bus. Each battery is managed by the BMI (Battery Management Interface) that, through 16 pins gateway, controls the intervention of the FAN for the battery cooling in case of high temperatures, the PWM of the on board own charger and the activation of the main switch in case of high voltage. As showed in Fig. 2, thanks to the Battery CAN, the six paralleled batteries communicate with the MBS (Multi Battery System), transferring information about temperatures, SoC and the operation of the

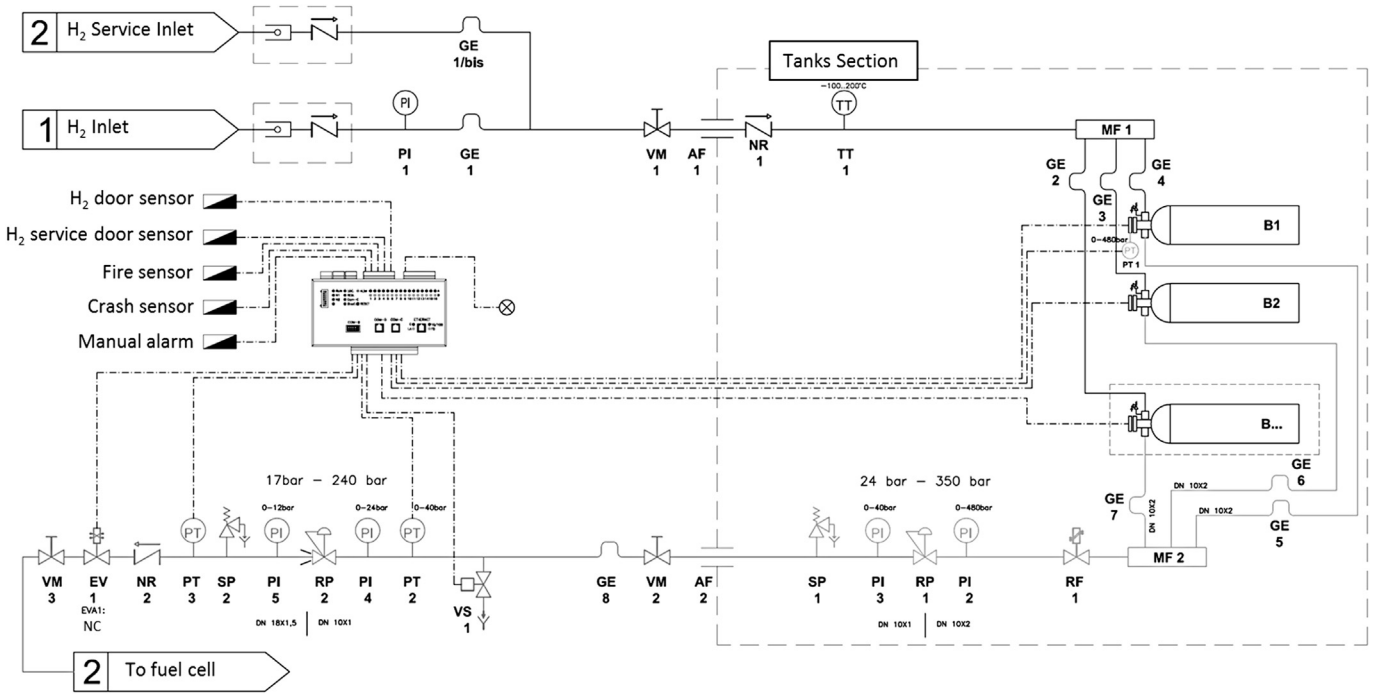

Fig. 7. Hydrogen storage system balance of plant.

battery pack. Vehicle CAN connects all principal devices with MC and MBS.

The city bus can be operated in hybrid mode (FC + batteries) or in pure electric mode (only batteries), through the activation of a selector on the dashboard.

This option was foreseen to avoid the FCS start-up when not necessary, for instance in the case of short routes (e.g. maintenance or parking in the depot). Furthermore, in the case of a breakdown of the FCS or DC/DC step-up converter, the bus can operate in pure electric mode, assuring the same reliability of an electric vehicle. It is clear that in this occurrence, the autonomy range of the vehicle is reduced, because the energy content in the hydrogen tanks is not available any longer.

Different active controls were foreseen. They start as soon as the bus is going to switch-on and expire when the bus is going to switch-off.

3.4. Faults detection

Depending on the type of error occurred the active controls can produce *Fault_Heavy* or *Warning* signals.

In case of *Warnings*, the state of the vehicle remains the current one, even if the warning information is transmitted to the driver display.

If a breakdown of such device in the chain among hydrogen storage system, FC system, and DC/DC Converter occurs, the result of the error is the lock of the tanks and hydrogen valves. This action determines automatically the deactivation of the FCS and DC/DC converter, because no energy could come from FCS. The vehicle can carry on the driving in pure battery mode and the MC generates a *Warning*, not a *Fault_Heavy*.

In case of *Fault_Heavy* the activation of the vehicle shut-down procedures starts.

The multiplex is dedicated to manage and control the part of the vehicle equipment not modified, including: subsystems, traction services, electric engine, auxiliary circuits and driver dashboard. Every error coming from these devices can be managed by the Multiplex, but in the case of the occurrence of a *Fault_Heavy*, MC needs to be informed. It manages and controls the hydrogen plant through analogue I/O.

The HSS is composed by 2 tanks and 3 decreasing stage of pressures, measured by tree pressure transmitters: high pressure (PT1), medium pressure (PT2) and low pressure (PT3) (Fig. 7).

The temperature is measured by sensors inside the tanks (VB1 and VB2). During hydrogen refuelling, if the temperature rises over the limit of 80 °C, a buzzer and a red light, close to the hydrogen inlet, are activated, alerting the refuelling operator. The hydrogen level is checked by a low pressure in the tanks (<50 bar → RESERVE on the HMI).

The check on the implemented devices is also defined, regarding both functionality and communications. Every device sends CAN messages with a known time interval; if no message comes from such device over the time defined, the MC performs a *Fault_Heavy* in the case of MBS and a *Warning* in the case of FCS and DC/DC Converter. A list of errors codes related to DC/DC Converter and FCS was implemented.

The 5.6 kW Proton Exchange Membrane stack (40 cells in series) is based on self-humidifying technology, so the water circuit works both for cooling and humidification. A general description of the stack and system can be found in Ref. [22].

Water formed in the cathode compartment is cooled by the use of a fan and a radiator, and condensed in the tank below the radiator. Then it is pumped in to the cathode input. 5 L of deionized water ($\sigma < 5$ μS) have to be loaded before starting. Hydrogen not used during the reaction is stored in the Recycle Tank and then recycled in the anode compartment through the output (difference pressure between input and output of the anode during the purging). Dedicated embedded control unit (ECU) and software drive the entire system for operations and safety. They acquire and elaborate information coming from the Cell Voltage Monitor (CWM), and from temperature, pressure and water level sensors. Leak of hydrogen is detected by a

hydrogen sensor: the ECU executes automatically the shut-down.

It is clear that a relevant number of error codes can derive from FCS through the Vehicle CAN, i.e. low or high hydrogen pressure, fill water tank, low cell voltage, hydrogen leak, low water temperature.

The logic implemented distinguishes among four cases to guarantee bus safety and functioning:

- Error codes that determine restarting the FCS.
- Errors codes that determine the Nuvera service. In this case the stack cannot operate.
- Error codes that determine the depot operator service. Probably it is possible to restart after the intervention.
- Error codes that can derive from malfunction of other devices (DC/DC Converter, auxiliary equipment, etc.). A technical intervention is mandatory, but the failure is not due to FCS.

Information about errors is shown on the HMI (Human Machine Interface), further it was foreseen a dedicated CAN gateway for diagnosis.

Similar logic is used for the battery management (*low SoC*, *low battery isolation*, *low temperature*). The error code coming from MBS can concern one or more batteries. Therefore, the information about the number of available batteries and their health is fundamental to understand the autonomy range and the traction performance of the bus.

3.5. Start-up

During the stop in the depot the vehicle is disable; only the Multiplex remains active.

As a matter of fact during the battery charging and the hydrogen refuelling MC needs to control:

- the on board chargers
- the hydrogen temperature and pressure

The switching on the bus is determined by the driver that turns the key (first impulse KeyC1). This action allows to supply with 24 V aux the HSS, DC/DC converter, FCS and HMI.

These devices begin to communicate with MC and the active controls are introduced.

When the driver turns the key for the second time (second impulse KeyC2) all the devices are activated, the Siemens engine included. The bus can be considered switched ON. At this step FCS is not already started.

If the driver has selected the hybrid mode, MC sends the CAN message to HSS (open valves) and to FCS to begin the start-up procedure. Even if the bus is able to move powered by only batteries, the driver has to wait the end of FCS warm-up in order to be sure of FCS health. Indeed, it is important to know the availability of hydrogen energy content before starting. The hydrogen tanks contain about 90 kWh of available energy. In the case of fault the bus shows a reduced autonomy.

3.6. Logic of the bus operating during running and shut-down

Both FC system and batteries contribute to the traction. During regenerative breaking the batteries are recharged by electric motor that in this situation works as generator. During every stop the full power of FCS is delivered to batteries.

When the vehicle reaches the terminal stop, even if it is impossible to move the vehicle because the electrical engine line is deactivated, the FCS continues to supply energy to battery pack (on board battery charge). This condition is very similar to that of an electrical charging station, even if in this case the energy is provided by the fuel cell system on board.

The shut-down procedures allow locking every process in safety. During shut-down the FCS needs to be supplied by 24 V aux vehicle batteries because the stack is going to switch off and the time needed can be even some minutes, during which the auxiliary services must to be active. A flow-chart is showed in Fig. 8.

4. Experimental: set-up tests

Several tests were performed to set-up the operating and the procedures of the bus. The tests concern from one hand the battery pack and the bus running in pure electric mode (the DC–DC converter is under development), from the other hand, the fuel cell system working on an electronic load to carry out the FC behaviour during start-up, warm-up, shut-down and normal operation.

4.1. Battery pack set-up tests

In Fig. 9 is reported the warm-up and charge phase of the single Z5 battery.

Data were acquired via CAN BUS through ZEBRA® monitor software and PCAN Explorer® software.

The figure shows the time needed to warm-up the battery up to 250 °C, starting from 25 °C, and the time needed to charge the battery from 20% SoC up to 100% SoC. At about 212 °C, the battery shows an OCV of 524.6 V. The battery charge begins at about 230 °C. The on board chargers regulate the charge of the battery through a Pulse With Modulation (PWM) managed by BMI. The slow charge, about 12 h, is achieved with currents from 5 A to 0 A, corresponding to SoC from 20% to 100%. At the end of charging phase, the battery shows an open circuit voltage of 565.7 V, even if, after a relaxing time period, it reaches the 558 V open circuit voltage.

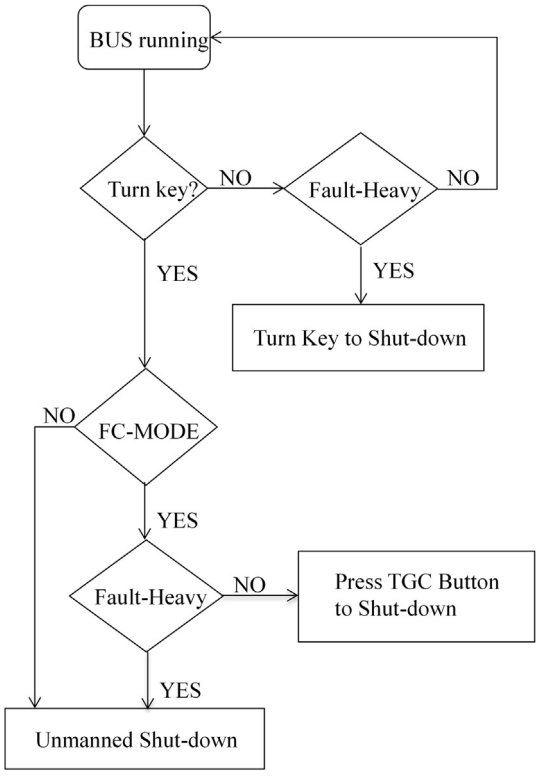

Fig. 8. Flow-chart of the shut-down logic.

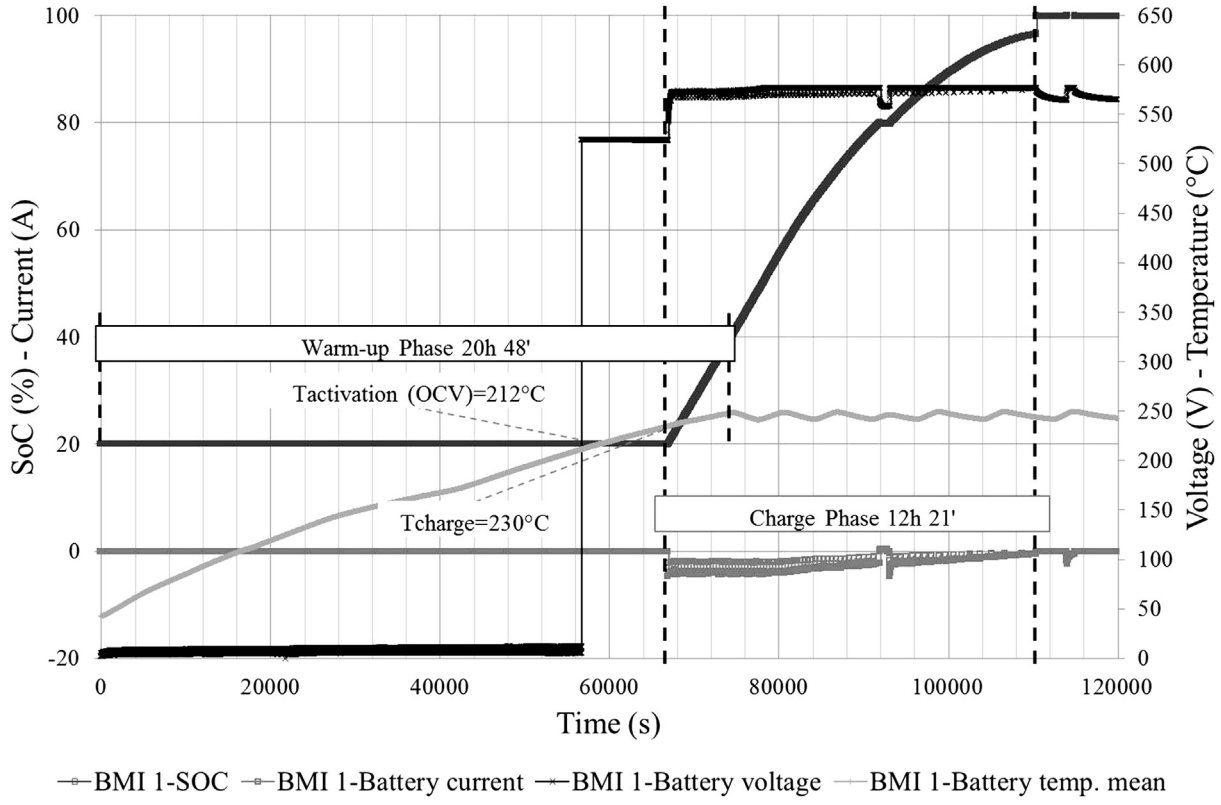

Fig. 9. Battery warm-up and charge phase.

First tests on running bus were performed in pure electric mode. The bus have run in an extra-urban route for 20 min without traffic and stops (Fig. 10).

The behavior of every single Z5 battery was recorded in terms of Voltage, Current and SoC.

The aim of this test was to verify the operating of battery pack during discharge and charge in regenerative breaking conditions and in general the power traction, in a real route.

The ΔSoC = 6% in a 20 min route (without the contribution of the fuel cell system) shown in Fig. 10, means about 7.56 kWh consumed. Evaluating the contribution in 20 min of the 5 kW PEM system of about 1.66 kWh (20 min at 5 kW constant power), the ΔSoC should be reduced at ΔSoC = 4.68%.

This trend (ΔSoC = 4.68% every 20 min route) confirms the good dimensioning and calculated autonomy of the bus because it allows a continuous operating up to 6 h, without considering stops, terminal stops and traffic.

Considering the parallel configuration of the battery pack, during the test every battery voltage was recorded and plotted versus the total electric engine power in order to verify possible voltage mismatches and ward off batteries charging from other batteries.

Fig. 11 shows that a good matching among the batteries voltages is present. Only during fast phases it was noticed some mismatches, from discharging to charging through regenerative breaking and vice versa, This can be considered a normal behaviour, because not significant differences of the resistance of the six paralleled electrical circuits, during the transients, determines a limited voltage variation (maximum 14 V), from the minimum to the maximum voltage recorded. In all other working points, the batteries voltages can be considered overlapping.

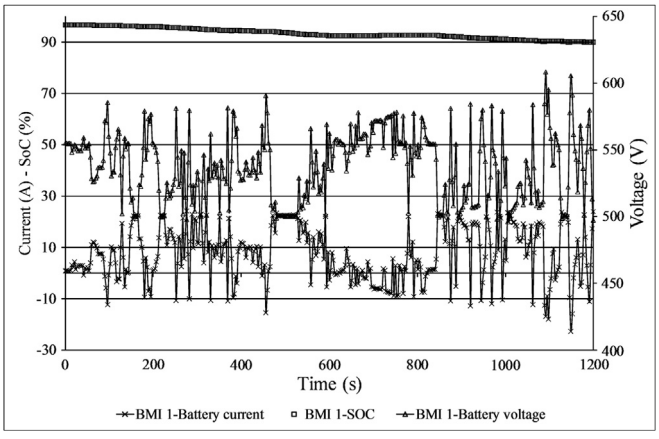

Fig. 10. Single Z5 battery behavior: 20 min route in pure electric mode.

4.2. Fuel cell system set-up tests

The 5 kW Power Flow of Nuvera® Fuel Cell was acquired and tested through a H&H® Electronic Load. Data were acquired via CAN BUS thanks to a data acquisition system (Power Flow System Monitor) provided by Nuvera.

In Fig. 12 is reported the start-up and warm-up of the fuel cell system where current, voltage, cathode temperature and power were recorded. During start-up procedure the fuel cell system is fed by an external power source (24 V Aux vehicle battery). Hydrogen and air flow through the stack powering the stack that shows an

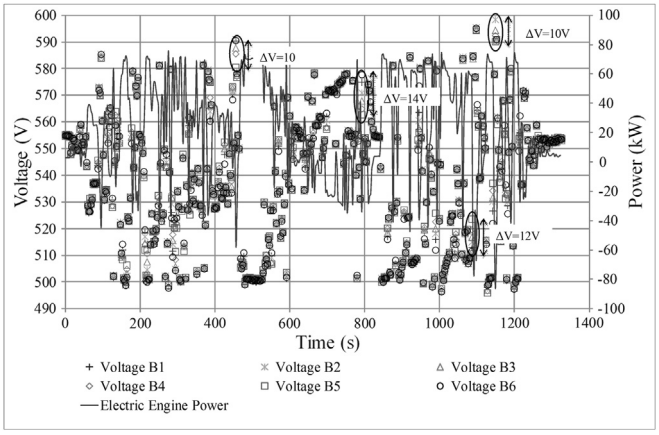

Fig. 11. Voltage mismatch among the batteries.

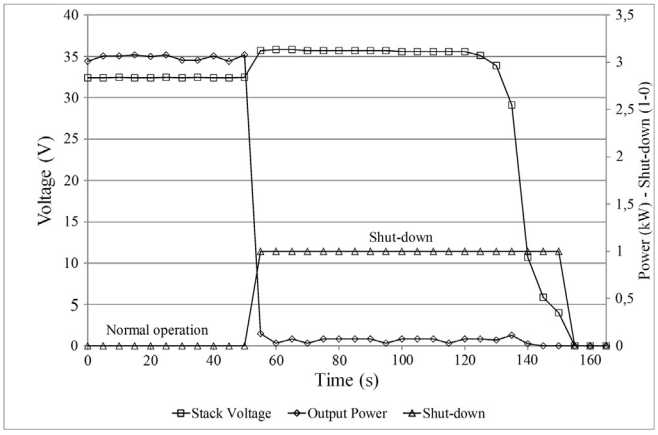

Fig. 13. Fuel cell system shut-down.

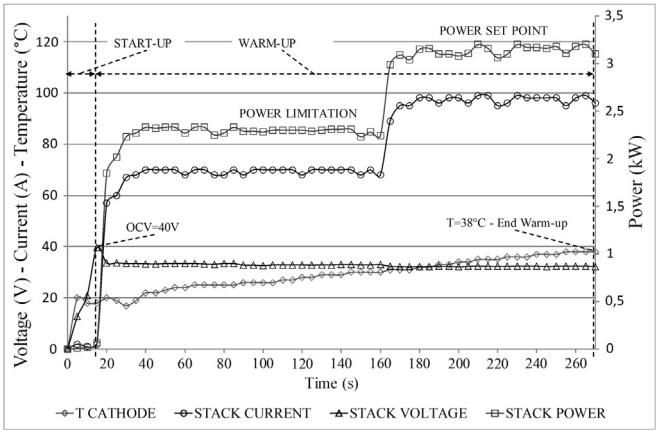

Fig. 12. Fuel cell system start-up and warm-up.

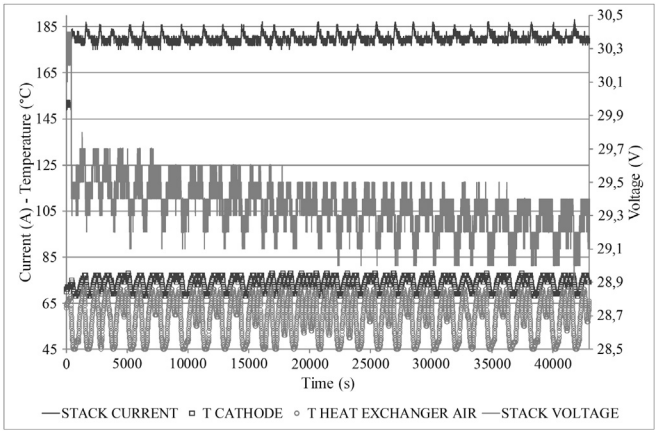

Fig. 14. Fuel cell stack behavior in continuous operation.

open circuit voltage of 40 V, after about 15 s. As soon as the water reaches a minimum target of 38 °C the membranes are considered sufficiently humidified. Depending on the initial water temperature and on the load current fed by the stack, the warm-up time can be more or less long. The higher the initial water temperature and load during warm-up, the less is the warm-up time. Even if a set point power of more than 3 kW was imposed during the test, the system limits the output power up to less than 2.5 kW. In order to minimize the warm-up period, the DC/DC step up converter control strategy was designed to set the output power of fuel cell system at 2.5 kW, the maximum power allowed during warm-up. During normal operation mode the system can supply the maximum power of 5.6 kW.

The fuel cell system shut-down time was measured in order to set-up the bus shut-down procedure (Fig. 13).

Fig. 13 reports that about 100 s are required to shut-down the fuel cell system. This time is very long compared with the conventional vehicles or with the pure electric vehicles. No solutions can be adopted to reduce this time because hydrogen has to be expulsed and the stack voltage has to reach zero voltage to consider the system switched-off and safe.

In order to analyze the stack behavior during a steady-state at maximum power (5.6 kW), the working point imposed by the bus control software, a long time test was performed.

The voltage variation of the stack voltage shown in Fig. 14 is due to consumptions of the ancillaries and in particular of the fan of the heat exchanger.

Every time the cathode temperature reaches about 78 °C, the fan starts determining a voltage drop and a current spike. The average voltage start from 29.5 V and reaches 29.2 V after 12 h of continuous operation.

This phenomenon is probably due to the water that during the operation of the stack occupies the catalytic sites and it is not well purged. It can be considered reversible because after a shut-down procedure the voltage level come back to the initial one. This variation is evaluated very short both in magnitude and dynamics.

5. Conclusion

The development of a hybrid urban bus, equipped with fuel cell and batteries, was carried out.

Although the DC–DC Converter is not still ready, the tests performed and reported in the paper on the fuel cell system (bench-tests) and on the battery pack (test on the running bus) have demonstrated the feasibility of the project and of the vehicle control strategy adopted. The powertrain management was tackled evaluating the vehicle and the possible meddling of human choice and automated procedures totally managed by Master controller. In both cases a HMI transmits, using a display, every message coming from MC (fault, warning, battery SoC, hydrogen fuelling need, etc.).

The start-up and shut-down procedures were designed in order to manage the long times required to warm-up and shut-down the fuel cell system.

The tests have confirmed the effectiveness of the powertrain designed and the capability of the reduced battery pack to drive the bus.

The stack behaviour, during 12 h of continuous operation, was analysed to assure a constant working point and consider possible voltage fluctuation due to the intervention of the ancillaries.

Comparing this vehicle to the battery-only vehicle version, the cost difference due to fuel cell and hydrogen storage system installed is limited at about 15%. So, the hybrid version cost is a little bit more than the only battery version.

This is due to the short size of fuel cell system adopted and due to the reduced battery pack.

This range-extender configuration proposed can now:

- reduce the number of vehicles needed in an electric buses fleet management, thanks to the fast refueling due to the hydrogen and to the extended autonomy
- facilitate the creation of a hydrogen vehicles early market thanks to the lower investment cost, compared with the full power one (total fuel cell vehicle)

Acknowledgements

The authors acknowledge the financial support of the Italian Ministry of Research. The authors are also grateful to Rampini Spa, Fiamm Spa, STMicroelectronics, SOL Group, Elton Electronics and Nuvera Fuel Cell for their contributions.

References

[1] J. Barkenbus, Policy Soc. 27 (2009) 399–410.
[2] C. Thiel, A. Perujo, A. Mercier, Energy Policy 38 (2010) 7142–7151.
[3] T.A. Becker, Electric Vehicles in the United States — a New Model with Forecasts to 2030, Center for Entrepreneurship & Technology University of California, Berkeley, 2009.
[4] P. Denholm, M. Kuss, R.M. Margolis, J. Power Sources 236 (2013) 350–356.
[5] J. Neubauer, A. Brooker, E. Wood, J. Power Sources 236 (2013) 357–364. http://www.sciencedirect.com/science/article/pii/S0378775312011809.
[6] J. Neubauer, A. Brooker, E. Wood, J. Power Sources 209 (2012) 269–277.
[7] J.J. Hwang, W.R. Chang, J. Power Sources 207 (2012) 111–119.
[8] C.H. Chao, J.J. Shieh, Int. J. Hydrogen Energy 37 (2012) 13141–13146.
[9] L. Andaloro, G. Napoli, F. Sergi, G. Dispenza, V. Antonucci, Int. J. Hydrogen Energy 38 (2013) 7725–7732.
[10] C.H. Dustmann, J. Power Sources 127 (2004) 85–92.
[11] T.M. O'Sullivan, C.M. Bingham, R.E. Clark, Zebra Battery Technologies for the All Electric Smart Car, in: International Symposium on Power Electronics, Electrical Drives, Automation and Motion, SPEEDAM, 2006.
[12] D.J.L. Brett, P. Aguiar, N.P. Brandon, R.N. Bull, R.C. Galloway, G.W. Hayes, K. Lillie, C. Mellors, C. Smith, A.R. Tilley, J. Power Sources 157 (2006) 782–798. http://www.sciencedirect.com/science/article/pii/S0378775306000516.
[13] R.C. Galloway, S. Haslam, J. Power Sources 80 (1999) 164–170.
[14] D.J.L. Brett, P. Aguiar, N.P. Brandon, J. Power Sources 163 (2006) 514–522.
[15] G.J. Suppes, S. Lopes, C.W. Chiu, Int. J. Hydrogen Energy 29 (2004) 369–374.
[16] G. Wang, J. Power Sources 196 (2011) 530–540.
[17] M. Ruth, M. Laffen, T.A. Timbario, Technical Report NREL/TP-6A1-46612, September 2009.
[18] S. Zhang, X.Z. Yuan, J. Ng, C. Hin, H. Wang, K.A. Friedrich, M. Schulze, J. Power Sources 194 (2009) 588–600.
[19] X.P. Wang, R. Kumar, D.J. Myers, Electrochem. Solid-State Lett. 9 (2006) A225–A227.
[20] H. Tang, Z.G. Qi, M. Ramani, J.F. Elter, J. Power Sources 158 (2006) 1306–1312.
[21] M.H. Rashid, Power Electronics Handbook, third ed., Butterworth-Heinemann – Elsevier, 2011.
[22] M. Ferraro, F. Sergi, G. Brunaccini, G. Dispenza, L. Andaloro, V. Antonucci, J. Power Sources 193 (2009) 342–348.